N89-20316

THE DYNAMICS OF FREE LIQUID DROPS

T. G. Wang, E. H. Trinh, A. P. Croonquist, and D. D. Elleman

Jet Propulsion Laboratory
California Institute of Technology

ABSTRACT

The behavior of rotating and oscillating free liquid drops has been studied by many investigators theoretically for many years. More recent numerical treatments have yielded predictions which are yet to be verified experimentally. The purpose of this paper is to report the results of laboratory work as well as of experiments carried out in space during the flight of Spacelab 3, and to compare with the existing theoretical studies. Ground-based experiments have been attempted as a first approximation to the ideal boundary conditions used by the theoretical treatments by neutralizing the overwhelming effects of the earth's gravitational field with an outside supporting liquid and with the use of levitation technology. The viscous and inertial loading of such a suspending fluid has been found to profoundly affect the results, but the information thus gathered has emphasized the uniqueness of the experimental data obtained in the low-gravity environment of space.

INTRODUCTION

The specific problems under consideration include experimental studies of the equilibrium shapes of drops in solid-body rotation, the shape oscillation spectrum of freely suspended liquids, and the interaction between rotation and vibration. The obvious difficulty in studying these phenomena dominated by the weak capillary forces is the presence of the earth's gravitational field. An experiment to be performed in the microgravitational environment of space was thus proposed and it has recently been carried out. This paper will describe the outcome of the operation of the Drop Dynamics Module[1] during the flight of Spacelab 3.[2] In order to obtain a more complete overview of the subject matter and to emphasize the need for a space experiment, the results of extensive ground-based studies will also be reported.

I. THE EQUILIBRIUM SHAPE OF ROTATING DROPS: THE PLATEAU EXPERIMENT REVISITED

A. Theoretical Background

Swiatecki[3] fits the problem of the liquid drop held together by surface tension into a broader scheme in which fluid masses may, in addition to having a surface tension, be self-gravitating and/or possess a uniform density of electric charge. The astrophysical problem of the stability of rotating stellar masses and the problem of the fissionability of rotating uniformly-charged nuclei are thus unified with the problem of equilibrium shapes and stability of ordinary liquid drops.

PRECEDING PAGE BLANK NOT FILMED

Confining discussion to the case of surface tension forces only, and assuming that the drop is actually confined within another fluid (e.g., a gaseous atmosphere) which rotates with the drop at the same angular velocity, the equilibrium shape must satisfy the Young-Laplace equation[4,5]

$$\Delta P_o + \frac{1}{2}\Delta\rho\Omega^2 r_\perp^2 = \sigma\,\nabla.\,n \tag{1}$$

The drop has density ρ_D and rotates with angular velocity Ω. The outer fluid has density ρ_F. The drop has a fixed volume. $\Delta P_o \equiv P_{D_o} - P_{F_o}$ is the difference in pressures on the axis of rotation inside and outside the drop, $\Delta\rho = \rho_D - \rho_F$ is the density difference, $r_\perp$ is the radius perpendicular to the axis of rotation and extending to the drop's surface, σ is the interfacial tension, and n is the surface normal ($-\frac{1}{2}\nabla.\,n$ is the local mean curvature).

Brown[6] rewrites equation (1) in the dimensionless form

$$Ha_o = K + 2\Sigma\left(\frac{r_\perp}{a_o}\right)^2 \tag{2}$$

where $H \equiv \frac{1}{2}\nabla.\,n$ is the local mean curvature, a_o is the radius of the sphere of same volume as the drop, and the parameters Σ and K are rotational Bond number and dimensionless reference pressure defined as

$$\Sigma \equiv \frac{\Omega^2\Delta\rho a_o^3}{8\sigma} \tag{3}$$

$$K \equiv \frac{\Delta P_o a_o}{2\sigma} \tag{4}$$

Figure 1 shows cross-sectional profiles of axisymmetric shapes for values of the reduced rotation rate squared, derived from reference 4. These cross sections lie in the meridional plane. The figures showing a dip at the axis are not lobed shapes, but are biconcave discs similar in form to red blood cells. The biconcave discs pinch off at $\Sigma = \frac{1}{2}$ and become tori ("tori" is used loosely to describe shapes which no longer intersect the axis of rotation).

A substantial extension to the theory to include the shapes and stabilities of nonaxisymmetric figures of equilibrium has been provided by Brown and Scriven[6]. Along the simply-connected sequence, the axisymmetric drop shape was shown to be stable to two-lobed perturbation for $\Sigma < 0.313$. At this point the drop is neutrally stable to these perturbations; above it, the axisymmetric shape becomes unstable. Similarly, as shown in Figure 2, Brown calculated bifurcation points to three- and four-lobed families from the simply-connected sequence at $\Sigma = 0.500$ and $\Sigma = 0.567$.

B. The Plateau Experiment Revisited

This experiment was first performed by Plateau[7] in the last century, and has been repeated at JPL using advanced photographic and electronic systems to achieve a better control of the various relevant parameters.[8]

A large (15 cc) viscous liquid drop is formed around a disc and shaft in a tank containing a much less viscous mixture having the same density. This supporting liquid and that of the drop are immiscible. If the shaft and disc were not present, the drop would float freely in the surrounding medium, and have the shape of a sphere. The gravitational forces are greatly reduced, and become small compared to the surface forces. With the drop attached and initially centered about the disc, the shaft and disc are set into rotation almost impulsively, reaching a final steady angular velocity within 1/2 to 2 revolutions. The drop deforms under rotation, and develops into a variety of shapes depending upon the shaft velocity. The process of spin-up, development, and decay (or fracture) to some final shape is recorded on motion picture film.

In this system, gravity is diminished at the expense of introducing a supporting liquid which is viscous, and which may be entrained by the motion of the drop, thereby allowing momentum to be transferred from the drop.[9] Rotation is achieved only by introducing the shaft and disc; adhesion to these surfaces distorts the drop shape. Nevertheless, comparison of this experiment's results to the theory of free rotating liquid drops is prompted by the fact that several novel families of drop shapes have been observed. It is important to recognize, though, that existing theories deal mainly with equilibrium shapes and their stability, while the drop in this experiment is undergoing a far more complicated process; the shape of a liquid drop spun from a shaft is a dynamical problem.

Plateau originally observed axisymmetric equilibrium shapes as well as tori when the rotation velocity was high enough. He found that the motion of the ring was that of a rigid body for several seconds. Most of Plateau's attention was devoted to the study of the rings which he thought were similar to the rings of Saturn.

The shapes observed in the JPL experiment were those of flattened, slowly rotating drops, as well as toroidal, two-, three-, and four-lobed shapes. Neutrally buoyant tracer particles allowed the study of the dynamics of the behavior, the secondary flow generated by the rotation, the interaction between the drop and the host liquid, and the coupling between the shaft/disc and the drop.

In the case of slowly rotating axisymmetric drops, comparison with the theory was possible and the resulting near-agreement was nevertheless remarkable: the qualitative shape of the equatorial area versus the reduced rotation rate were similar, only differing from theory by 30%. When generating $n>2$ lobed drops in a controlled manner, primarily two- and three-lobed shapes were obtained. The latter had not been observed

before. The behavior of the lobed shapes was not easily compared with theory, however. The study of the angular velocities and momenta demonstrated that the development of the various lobed shapes takes similar paths, but no evidence was found for the location of the branch points between axisymmetric and triaxial behavior. Figure 3 reproduces photographs of some of the drop shapes obtained.

C. Ground-Based Studies of Rotating Charged Drops

The investigation of the behavior of rotating charged drops under the full effect of the earth's gravitational field has been made possible by electrostatic and acoustic levitation technologies. A small (3-4 mm in diameter) charged liquid drop could be electrostatically levitated and acoustically rotated.[10] The first bifurcation point marking the transition from axisymmetric to two-lobed shape was accurately observed. The detailed analysis revealed the action of gravity in the geometry of the drop. The theory is not applicable to a nonuniform charged drop, and the stability of the equilibrium shape must be greatly modified by the electrostatic stresses at the drop boundary.

II. THE DYNAMICS OF SHAPE OSCILLATIONS OF FREE DROPS: LABORATORY EXPERIMENTS

A. Theoretical Background

Extensive theoretical work exists on the subject of drop shape oscillations.[11-19] Miller and Scriven[17] have produced a comprehensive theoretical analysis of the natural, small amplitude, shape oscillations of a drop by using the normal-mode approach. Marston[18] has offered a derivation for the case of a liquid drop immersed in another liquid of similar properties. Prosperetti[16] has obtained a solution to the initial value problem and has provided theoretical predictions concerning the behavior of a freely oscillating drop in the early transient period.

An expression for the L_{th} resonant mode frequency of a driven oscillating drop is given by

$$\omega_L = \omega_L^{\bullet} - \frac{1}{2}\alpha\,\omega_L^{\bullet} + \frac{1}{2}\alpha^2, \tag{5}$$

where ω_L is the angular response frequency, and ω_L^{*} is Lamb's natural resonance frequency.[11]

$$\left(\omega_L^{\bullet}\right)^2 = \frac{L(L+1)(L-1)(L+2)}{R^3[L\rho_o + (L+1)\rho_i]}\sigma \tag{6}$$

R is the radius of the undisturbed spherical drop, σ is the interfacial tension, and ρ_i and ρ_o are the density of the inner and outer fluid respectively.

α is given by

$$\alpha = \frac{(2L+1)^2(\mu_i\mu_o\rho_i\rho_o)^{\frac{1}{2}}}{\sqrt{2}\,R[L\rho_o+(L+1)\rho_i][(\mu_i\rho_i)^{\frac{1}{2}}+(\mu_o\rho_o)^{\frac{1}{2}}]} \tag{7}$$

μ_o and μ_i being the dynamic viscosity of the two liquids.

The free decay of an oscillating drop is given by the damping constant τ_L^{-1}

$$\tau_L^{-1} = \frac{1}{2}\alpha\,\omega_L^{\frac{1}{2}} + \frac{1}{2}\Gamma - \frac{1}{2}\alpha^2 \tag{8}$$

where

$$\Gamma = \frac{(2L+1)\left\{2(L^2-1)\mu_i^2\rho_i + 2L(L+1)\mu_o^2\rho_o + \mu_i\mu_o[(L+2)\rho_i-(L-1)\rho_o]\right\}}{R^2[(\mu_i\rho_i)^{\frac{1}{2}}+(\mu_o\rho_o)^{\frac{1}{2}}]^2[L\rho_o+(L+1)\rho_i]} \tag{9}$$

The first term in the expression for the damping constant [equation (8)] expresses the damping in the oscillating boundary layer of the drop, while the second term reflects the dissipation mechanism due to viscous effects within the drop itself and is equivalent to the damping normally associated with the well-known harmonic oscillator.

These results are valid under the assumptions of small-amplitude oscillations, vanishing tangential stresses at the drop boundary, and the absence of internal circulation. No dependence of the resonance frequencies on the oscillation amplitude can be derived, and the various modes are assumed to be decoupled. One may notice that each normal mode denoted by the integer L is actually degenerate in the axisymmetric case. For example, for the $L=2$ mode, there exist five degenerate modes corresponding to the integer values $m = \pm 2, \pm 1, 0$, all having the same frequency, but differing by the geometry of their oscillations.

Foote[15] has carried out computer calculations without the restriction of small-amplitude oscillations and has determined that the frequency of each normal mode decreases with increading oscillation amplitude. In addition, his results indicate that for the $L=2$ mode, the drop spends more time in the prolate configuration than in the oblate one. Tsamopoulos and Brown[19] have obtained similar results for the oscillation frequency.

Busse[20] has carried out an asymptotic expansion analysis of the problem of the oscillation dynamics of a rotating drop in the small oscillation amplitude region.

B. Ground-Based Experiments

Novel acoustic levitation techniques have allowed the study of the oscillatory behavior of freely suspended drops both in an immiscible liquid system as well as with liquid suspended in a gaseous atmosphere.[21-26] The detailed experimental investigation of the small-amplitude shape

oscillation of liquid drops suspended in an immiscible liquid host has allowed the verification of theoretical results.[21] Figure 4 presents a series of photographs of the first three pure resonant modes of shape oscillation of an acoustically levitated and excited drop. Heretofore undetermined experimentally, the resonance frequencies of these modes were accurately measured and closely correlated with the calculated values. Table I reproduces the results of the comparison between experimental and theoretical values. In the same manner, the decay rate of the fundamental mode has been accurately measured and compared with the theory. The results are summarized in Table II.

Nonlinear effects were also experimentally studied as drops could be driven into high-amplitude oscillation with modulated acoustic radiation forces. A markedly soft nonlinearity was observed for freely decaying drops as the data reported in Figure 5 illustrate. Tsamopoulos[19] compared these data with his computer calculations, and found good agreement. The case for driven drops is more complicated, however, because of the subtle effect of the static shape on the oscillatory modes: the resonant modes of a slightly oblate drop have been found to increase as the level of deviation from sphericity was increased, an effect until now unreported.[21-23] Flow visualization studies of the internal fluid particle motion within an oscillating drop have revealed a qualitative change in the flow pattern as the oscillation amplitude grows: vorticity not present in the small-amplitude region exists in each of the quadrants of a drop under quadrupolar vibration. Figure 6 reproduces some of the photographs obtained from tracer particles illuminated with sheet lighting. The streak pattern is obtained through a time exposure lasting several oscillation cycles.

Experiments using smaller (4 mm diameter) drops levitated in air have also yielded similar soft nonlinearity for driven large-amplitude oscillation. Similarly, the resonant modes of oscillations have been experimentally investigated for a drop in solid-body rotation, freely suspended in an immiscible host liquid and restrained by an ultrasonic field. Sample results are reproduced in Figure 7. The relative shift in the resonance frequency has been plotted as a function of the ratio of the rotation velocity to the angular resonant frequency of the nonrotating drop. Very good agreement with the theory[24] has been discovered for the fundamental mode. An intriguing experimental observation was provided by the multiplicity of resonant modes as the rotation rate was increased: it appeared that the rotation removed the degeneracy of the fundamental mode. Such evidence correlates with observations of frequency shift of the oscillation modes of the sun due to its rotation. The physical processes in that particular case are more complicated due to the differential rotation.

III. SPACELAB 3 DROP DYNAMICS EXPERIMENTS

A. Introduction

The video downlink from the Space Shuttle Challenger on May 3, 1985, displayed a liquid drop being held and manipulated within a seemingly invisible container. This was the first live demonstration in the microgravitational environment of space of the capabilities of acoustic radiation forces: a resonant cavity confining three-dimensional standing waves was used to create a stable potential well to position, rotate, and oscillate a liquid sphere. Promising future applications of such techniques may be found in space where the reduction of the effects of gravity allows the effective use of relatively small forces to manipulate materials samples without interfering with their behavior and thereby introducing extraneous artifacts.

The purpose of this first set of experiments in Spacelab was the investigation of the rotational and oscillatory dynamics of free liquid drops under the subtle influences of surface tension and acoustic radiation pressure forces. The specific goals were to test the capabilities of acoustic manipulation techniques, to gather the first experimental data on the equilibrium shapes of rotating free liquid drops, and to demonstrate the capability of drop oscillation techniques for the measurement of the surface tension and viscosity of liquids. All experiments were carried out at ambient temperature and in the Spacelab atmosphere. Data were primarily obtained in the form of 16 mm cinefilms. Each frame of the film was divided into four subframes, three of these contained views of the drops along three orthogonal axes, and the fourth quadrant was devoted to the display of data relating to the operation of the instrument. The bulk of the engineering data was recorded on magnetic tapes.

B. Acoustic Positioning and Torque Applied to Liquid Drops in Microgravity

Available experimental evidence appears to indicate that the steady-state acceleration levels in the Spacelab 3 module during a gravity gradient attitude is on the order of 0.001 g (where g is the gravitational level at sea level on earth) with occasional deviations reaching amplitudes up to 0.1 g. Our observations reveal that the acoustic positioning forces generated in the experiment chamber (DDM chamber) were capable of containing a 7 cc liquid drop having a density of 1.18 g/cc when subjected to the steady-state level of residual acceleration, but were unable to restrain liquid drops during spacecraft maneuvers characterized by peak acceleration levels of 0.1 g. Figure 8 is a plot of the maximum acoustic force generated at four different sound pressure levels (140, 143, 146, and 149 dB re. 0.0002 microbar) as a function of the drop volume. The 7cc drop mentioned above would thus require an SPL of about 143 dB for trapping within the acoustic potential well. The drop was observed, however, to remain near the center of the chamber for long periods of time during which the sound level was

significantly lower than 143 dB, thus suggesting that the steady-state acceleration level might be lower than 0.001 g for those periods of time.

The acoustic restoring force in a one dimensional standing wave may be expressed as[27]

$$F = \frac{5\pi}{6}\left(\frac{P_i^2}{\rho c^2}\right) k R^3 \sin 2kx, \tag{10}$$

where ρ_i is the pressure amplitude, ρ and c are the density and sound velocity characteristic of air, k is the wave vector, and R is the radius of a spherical sample. Theoretically, the restoring force is reduced to zero at the center of the chamber, and increases sinusoidally as the sample deviates from that position. In practice, the force profile is not sinusoidal, and is fairly distorted due to scattering effects from the sample.

During the operation of the experiment, the acoustic pressure levels were maintained between 135 and 145 dB and little static distortion of the drop was observed during normal operating sequences. This absence of static, acoustically induced distortion is crucial to the viability of acoustical manipulation techniques as experimental tools for materials science and fluid dynamics investigations.

Should a freely suspended drop receive an impulse from a transient acceleration spike, it will undergo translatory oscillations within the potential well controlled by the acoustic restoring force. The frequency of this oscillatory motion may be used to estimate the magnitude of this restraining force if the drop mass is known.

When two sides of the acoustic resonant cavity have equal length, it is possible to generate a steady-state torque by means of appropriate phasing of the associated acoustic waves. When the two waves along the x and y axes are related by $+90°$ (or $-90°$), a torque with direction vector in the $+z$ (or $-z$) direction is induced and drives a clockwise (counterclockwise) rotation of a sample suspended in the center of the chamber. The theoretical expression for this torque is given by[28]

$$T = \frac{3}{2} L_\eta \frac{P_x P_y}{2\rho c^2} \mathrm{A} \sin \phi_o, \tag{11}$$

where T is the torque, L_η the acoustic boundary layer (or viscous length) defined as $(2\nu/\omega)^{\frac{1}{2}}$, P_x and P_y the pressure amplitudes of the waves in the x and y direction respectively, A the total surface area of the sample, ν the kinematic viscosity of the air, ω the angular frequency of the sound wave, and ϕ_o the phase angle between the waves along the x and y axes.

By knowing the torque acting on the liquid drop, the deformation of the drop as it rotates, and the drag of coefficient of the air, it is possible to plot the rotation rate of a given sample as a function of time. The results of such a calculation are reported in Figure 9 for a 3 cc drop of water/glycerin

mixture with a kinematic viscosity of 100 centiStokes. The theoretical curve has been obtained by fitting the experimental data with the air drag coefficient as an adjustable parameter. The data included in Figure 9 pertains to a drop having a shape axisymmetric with respect to the axis of rotation.

C. Equilibrium Shapes of Acoustically Rotated Drops

As an initially spherical liquid drop is rotated around a fixed axis, its equilibrium shape has been predicted[3] to first remain axisymmetric with respect to the rotation axis. However, as the rotation rate is further increased, a sudden transition to a two-lobed shape will take place at a well-defined rotation speed. This transition point, commonly referred to as a bifurcation point, marks the limit of stability of the axisymmetric shape in favor of the two-lobed configuration. Numerical computations[4] have also predicted the existence of three- and four-lobed shapes appearing at higher rotational velocities. These higher order lobed shapes, however, are not stable configurations. For an isolated drop, the two-lobed configuration is the only stable equilibrium shape as the first bifurcation point is passed.

Figure 10 reproduces the experimentally measured rotation velocity of a 3 cc water/glycerin drop as the acoustic torque is applied and removed. The horizontal axis displays time. As the drop is spun up, it flattens at the pole and bulges at the equator, remaining axisymmetric and gaining in rotation speed. At the bifurcation point, the two-lobed shape becomes the stable equilibrium geometry and the drop slows down because the moment of inertia increases as well as the surface area. Although the speed decreases, the largest dimension of the drop cross section continues to increase, leading to an eventual fission of the liquid into two separate drops. In this particular case, however, the data of Figure 10 show that the acoustic torque is turned off before fission is allowed to occur, and the rotation speed increases again as the drop-stretch is reversed. The axisymmetric equilibrium shape is recovered when the same rotation speed as that measured at bifurcation during the spin-up phase is reached. No "hysteresis" has been detected within the present experimental uncertainty.

Due to imperfect conditions in the lighting system, the quality of the images recorded on the 16 mm films were slightly degraded, affecting the precision with which the drop shape and speed could be measured. As a result, measurements of the relative change in the drop cross section and profile could be accomplished with an uncertainty of about $\pm 8\%$. The rotation velocity of the drop was measurable to within $\pm 5\%$.

A plot of the axial ratio of the spheroidal drop in the axisymmetric regime is reproduced in Figure 11. The drop profile has been measured with images recorded on views along axes perpendicular to the rotation axis. The drop deformation is plotted as a function of the rotation velocity.

Figure 12 presents the experimental data together with available theoretical predictions. In this case, the largest dimension in the rotating drop equatorial cross section (measured perpendicularly to the rotation axis) divided by the radius of the nonrotating drop, is plotted as a function of the rotation rate divided by the frequency of the fundamental mode of shape oscillation. This frequency is given by

$$F = \frac{1}{2n}\left(\frac{8\sigma}{\rho^* R^3}\right)^{\frac{1}{2}} \tag{12}$$

where σ is the surface tension of the liquid and ρ^* its density. The liquids used in these experiments were water, a series of water and glycerin mixtures of increasing viscosity (from 10 to 500 cSt), and finally silicone oil. The density was between 1.0 and 1.18 g/cc, and the surface tension had values between 20 and 70 dynes/cm.

The results in Figure 12 have been obtained with a 100 cSt liquid drop 3 cc in volume, and using rotational acceleration of about 0.01 revolution/sec. Under these particular circumstances, solid-body rotation is easily attained, and the effects of differential rotation are minimized. The behavior of the drop should then approach that of a fluid mass rotating at constant velocity since the rotation rate changes very little during the characteristic time required for reaching solid-body rotation. This assumption would not be valid if the viscosity were significantly lower.

The data reveal very good agreement with the theoretical predictions corresponding to the axisymmetric regime. On the other hand, a quantitative confirmation of the theoretical prediction was not obtained for the specific value of the reduced rotation rate at the bifurcation point. Experimental evidence suggests that the onset of secular instability for the axisymmetric shape is located at a lower rotational velocity than that predicted theoretically.

Figure 13 reproduces both experimental and theoretical results for an experimental sequence including a drop fission. Once again qualitative agreement is obtained, but the experimental data reveal a much faster increase in deformation with the decrease in rotation velocity. Fission generally produces two main drops of equal volume and a satellite droplet arising from the breakup of the liquid bridge forming the central region of the stretched rotating single drop. Assessment of the volumes of the drops resulting from fission is difficult to obtain, but their volumes were probably equal to within 10%. No evidence for two-lobed configurations with greatly differing volume for the lobes has been obtained.

D. Shape Oscillations and Measurement of Surface Tension and Viscosity

The portion of the experiment dealing with shape oscillation studies has been curtailed due to a subnominal performance of phase control which resulted in the inability to completely null out the acoustic torque. It was

nevertheless possible to obtain free decay measurement of the frequency and damping of shape oscillations as a means for determining the surface tension and viscosity.

Figure 14 reproduces the experimental results obtained for a freely decaying 4.5 cc drop of water/glycerin mixture having a viscosity of 10 cSt. A fit of the experimental data using an exponentially decaying sine wave yielded a surface tension of 60 dynes/cm and a viscosity of 12 cSt. The experimental uncertainty is primarily due to the relatively low frame rate used for the 16 mm camera.

Nonlinear effects arising during large amplitude oscillations of the drops were among the unfulfilled experimental goals due to lack of operation time as well as subnominal control over the nulling of the acoustic torque. Ground-based experiments[5] using immiscible liquid systems have suggested a soft nonlinearity in the resonance frequencies for shape oscillations as the amplitude grows large. The scant data available from this flight do not appear to confirm this finding, but suggest the existence of a hard nonlinearity. The results are very inconclusive, however, and these experiments must be repeated in possible subsequent flights. Additional phenomena to be studied in the future include the oscillatory dynamics of a rotating drop, the behavior of a compound drop, and the detailed behavior of particles inside a rotating and oscillating drop.

Preliminary observations concerning the last item mentioned above have demonstrated the ability to separate different phases present inside a liquid drop by simple rotation. Immiscible liquid droplets initially uniformly distributed within the main drop were quickly gathered at the center during rotation. The droplet density was 15% lower than the main drop density, and the centering process took approximately 2 minutes with rotation rate increasing from zero to about 2 revolutions/sec. An air bubble having diameter on the order of a millimeter and injected within the main drop only took 30 seconds to migrate to the center when the drop was accelerated from zero to 0.24 revolution/sec.

CONCLUDING REMARKS

Although certain ones of the planned experiments dealing with the oscillatory behavior of free drops could not be fully completed, and some of the precision of the measurement capability of the instrument was compromised by hardware malfuction, a very needed and successful test of the capabilities of acoustic positioning and manipulation techniques was carried out, an experimental confirmation of the theory of acoustic torque has been obtained with deformable liquid samples, the first set of data on the equilibrium shapes of rotation drops has been gathered to partially confirm available theories, and finally a successful demonstration of the contactless method of measuring surface tension and viscosity has been obtained. As is usually the case in experimental science, however, additional data must be obtained in order to confirm the results of this first flight.

It must be reiterated that the availability of a greatly reduced gravitational acceleration condition is essential to the rigorous performance of this experiment. This seemingly simple problem involves boundary conditions which are theoretically simple, but which are an earthbound experimentalist's nightmare. A neutral buoyancy system may be used to remove the effects of the gravitational field, but the host liquid alters the boundary conditions through viscous and inertial stresses. Levitation of free drops in a gaseous atmosphere on earth introduces non-negligible drop distortion as well as artifacts due to the levitating acoustic or electrical fields.

ACKNOWLEDGMENTS

The research described in this paper was carried out at the Jet Propulsion Laboratory, California Institute of Technology, under contract with the National Aeronautics and Space Administration.

REFERENCES

1. T. G. Wang, M. M. Saffren, and D. D. Elleman, "Acoustic Chamber for Weightless Positioning," AIAA paper, 74-155 (1974).
2. T. G. Wang, E. H. Trinh, A. P. Croonquist, and D. D. Elleman, "The Shapes of Rotating Free Drops: Spacelab 3 Experimental Results," Phys. Rev. Lett. (1986).
3. W. J. Swiatecki, "The Rotating, Charged, and Gravitating Liquid Drop and Problems in Nuclear Physics and Astronomy," Int'l. Colloquium on Drops & Bubbles, Proceedings, M. M. Saffren, D. Collins, Eds., Pg. 52, (1974).
4. S. Chandrasekhar, Proc. Roy. Soc. London, 286, 1, (1965).
5. D. K. Ross, Aust. J. Phys. 21, 823, (1968).
6. R. A. brown and L. E. Scriven, Proc. Roy. Soc. London, 371, 331, (1980).
7. J. Plateau, "Experimental and Theoretical Researches on the Figures of Equilibrium of a Liquid Mass Withdrawn From the Action of Gravity," Annual Report of the Board of Regents of the Smithsonian Institution, p.207, (Government Printing Office, Washington, DC, 1963).
8. R. Tagg, L. Cammack, A. Croonquist, and T. G. Wang, "Rotating Liquid Drops: Plateau's Experiment Revisited," JPL Publication 80-66 (1980).
9. E. H. Trinh, T. G. Wang, and M. C. Lee, "A Technique for the Study of Drop Dynamics in Liquid-Liquid Systems," J. Acoust. Soc. Am., 67 (1980).
10. W. K. Rhim, S. K. Chung, E. H. Trinh, and D. D. Elleman, "Charged Drop Dynamics Experiments Using an Electrostatic-Acoustic Hybrid System," Proc. Mat'ls. Research Soc. Symp. on Microgravity (Boston) (1986).
11. H. Lamb, Hydrodynamics, 6th Edition, Cambridge Univ. Press, 473, (1932).
12. Lord Rayleigh, The Theory of Sound, Dover, NY, 371, (1945).
13. W. H. Reid, Quart. Appl. Math., 18, 86, (1960).
14. S. Chandrasekhar, Hydrodynamic and Hydromagnetic Stability, Oxford Univ. Press (1961).
15. G. B. Foote, "A Theoretical Investigation of the Dynamics of Liquid Drops," PhD Thesis, Univ. of Arizona, (1971).
16. A. Prosperetti, J. Fluid Mech., 100, 333, (1980), and J.Mechanique, 19, (1980).
17. C. Miller and L. Scriven, J. Fluid Mech., 32, 417, (1968).
18. P. Marston, J. Acoust. Soc. Am., 67, 15, (1980).

19. J. Tsamopoulos and R. Brown, J. Fluid Mech., 127, 519, (1983).
20. F. Busse, J. Fluid Mech., 142, 1, (1984).
21. E. H. Trinh, A. Zwern, and T. G. Wang, "An Experimental Study of Small Amplitude Drop Oscillations in Immiscible Liquid Systems," J. Fluid Mech., 115, 453, (1982).
22. E. H. Trinh and T. G. Wang, "Large Amplitude Drop Shape Oscillations: An Experimental Approach," J. Fluid Mech., 122, 315, (1982).
23. E. H. Trinh, IEEE Proceedings in Ultrasonics, vol. 2, 1143, (1983).
24. E. H. Trinh and T. G. Wang, Proceedings of the Second Int'l. Colloquium on Drops and Bubbles, D. H. LeCroissette, Ed., JPL Publications 827, 143, (1981).
25. P. Annamalai, E. H. Trinh, and T. G. Wang, "Experimental Study of the Oscillations of a Rotating Drop," J. Fluid Mech, 158, 317 (1985).
26. E. H. Trinh and T. G. Wang, "A Quantitative Study of Some Nonlinear Aspects of Drop Shape Oscillations," J. Acoust. Soc. Am. 68, (1980).
27. E. Leung, N. Jacobi, and T. G. Wang, "Acoustic Radiation Force on a Rigid Sphere in a Resonance Chamber," J. Acoust. Soc. Am. 70, 6, (1981).
28. F. G. Busse and T. G. Wang, "Torque Generated by Orthogonal Acoustic Waves - Theory," J. Acoust. Soc. Am. 69, (1981).

TABLE CAPTIONS:

Table I Comparison of experimental results with theoretical calculations for the first four resonant modes of shape oscillations.

Table II Comparison of experimental results with theoretical calculations for the damping constant of the fundamental resonant mode of shape oscillations.

FIGURE CAPTIONS:

Figure 1: Axisymmetric equilibrium shape according to Chandrasekhar's results.

Figure 2: Predicted bifurcation points from axisymmetric to multi-lobed shapes according to the results of Brown.

Figure 3: Equilibrium shapes of rotating drops obtained in the JPL Plateau experiment.

Figure 4: Photographs of silicone oil drops oscillating in water. The first three resonant modes are shown (from ref. 21).

Figure 5: Experimental results for the frequency shift at high amplitude oscillation for the fundamental mode (from ref. 22).

Figure 6: Streak patterns photographs of suspended tracer particles in silicone oil drops levitated in water and oscillating in the fundamental mode at increasingly larger amplitude (from ref. 22).

Figure 7: Relative frequency shift of the second resonant mode of shape oscillation for a rotating drop levitated in water as a function of the square of the reduced rotation rate. (from ref. 25).

Figure 8: Maximum acoustic force at 1kHz and for four different sound prssure levels (SPL in dB re. 0.0002 microbar).

Figure 9: Rotation rate of axisymmetric drops. Theoretical fit for drop spin-up.

Figure 10: Axisymmetric and two-lobed regions of rotating drop.

Figure 11: Axial ratio of axisymmetric rotating drop.

Figure 12: Comparison of experimental with theoretical results for a 100 cSt. liquid drop.

Figure 13: Experimental data for drop fission due to rotation.

Figure 14: Free decay of shape oscillation.

	f_2 (Hz)	f_3	f_4	f_5	$\frac{f_3}{f_2}$	$\frac{f_4}{f_2}$	$\frac{f_5}{f_2}$	
Silicone/CCl_4 water, 3.2cst. 1.9 cm^3	3.56 (±0.07)	6.49 (±0.13)	9.37 (±0.19)	13.1 (±0.25)	1.82 (±0.07)	2.63 (±0.1)	3.67 (±0.15)	Experimental
					1.89	2.89	3.99	Lamb's formula
					1.82	2.64	3.69	Theory (Marston)
Silicone/CCl_4 in water, 3.2 cst. 1.7cm^3	3.66	6.81	10.21	13.65	1.86	2.79	3.73	Experimental
					1.86	2.79	3.74	Theory
Silicone/CCl_4 in water, 3.2 cst. 1.5 cm^3	3.87	7.21	10.45		1.86	2.70		Experimental
					1.86	2.81		Theory
Phenetole in water/Methanol 1.2 cst. 1.5 cm^3	2.97	5.54	7.85	10.47	1.87	2.65	3.52	Experimental
					1.85	2.90	3.65	Theory

TABLE I

Inside Viscosity	Outside Viscosity	Damping Constant (sec^{-1})	
1.05 cst.	10 cst.	1.52 (±0.1)	Experiment
		1.16	Marston Theory
1.05 cst.	20 cst.	2.93 (±0.15)	Experiment
		3.66	Theory
16.5 cst.	1.1 cst.	1.58 (±0.1)	Experiment
		1.82	Theory
36.8 cst.	1.1 cst.	2.63 (±0.15)	Experiment
		3.1	Theory

TABLE II

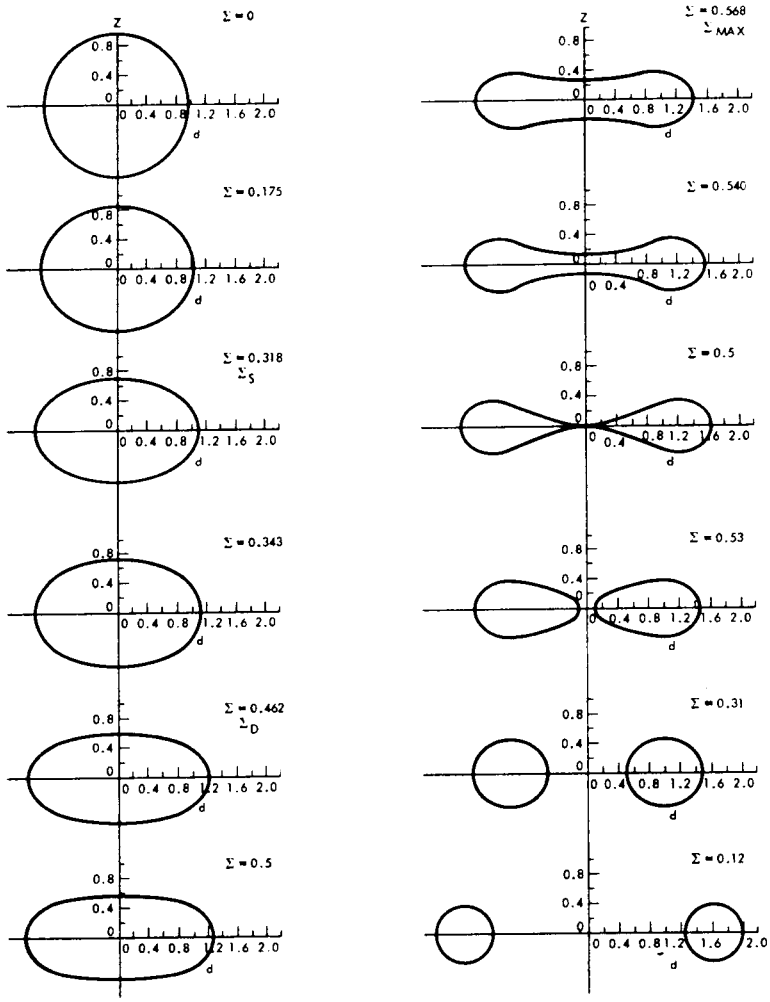
Σ = 0
Σ = 0.175
Σ = 0.318
Σ = 0.343
Σ = 0.462
Σ = 0.5
Σ = 0.568
Σ = 0.540
Σ = 0.5
Σ = 0.53
Σ = 0.31
Σ = 0.12
Z
d

Figure 1

ORIGINAL PAGE IS
OF POOR QUALITY

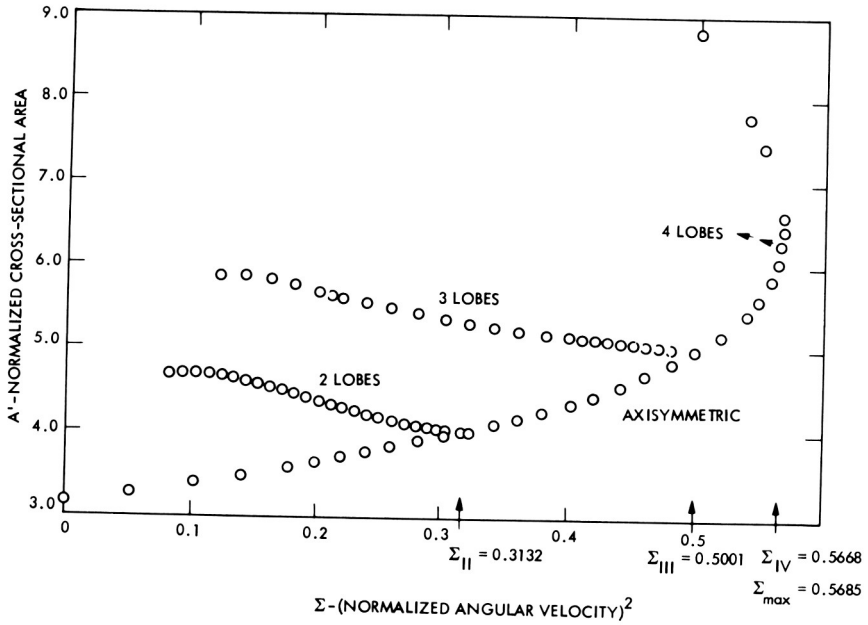

Figure 2

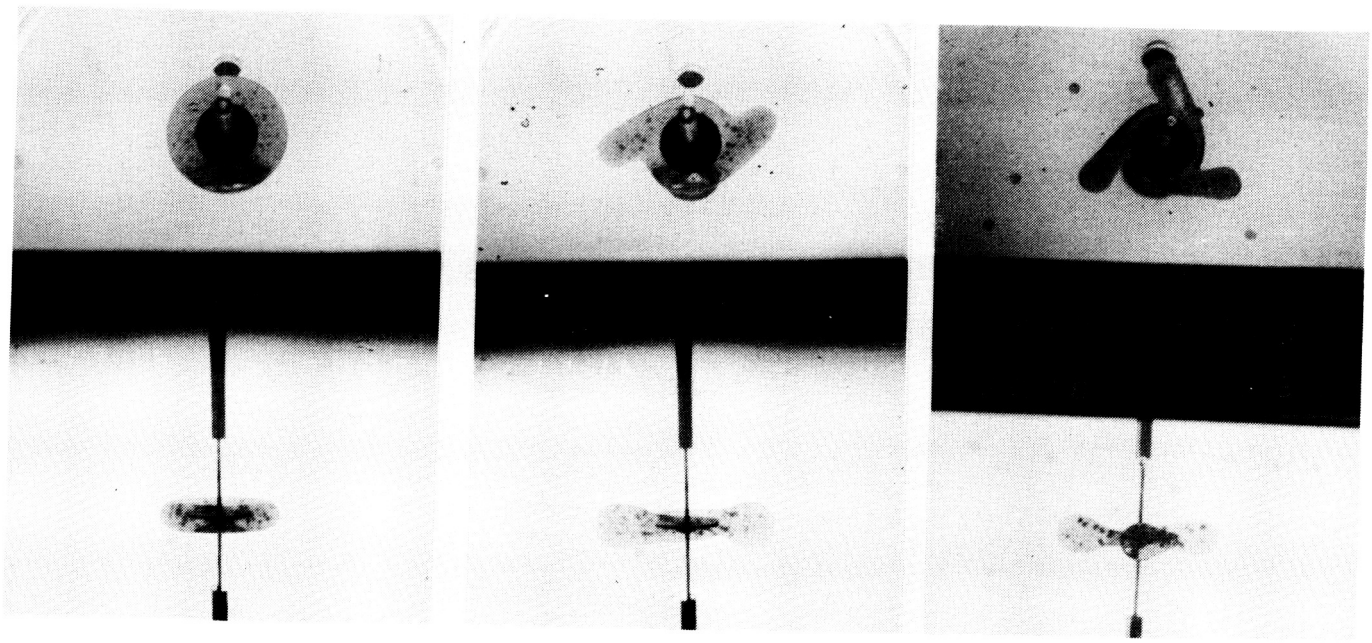

Figure 3

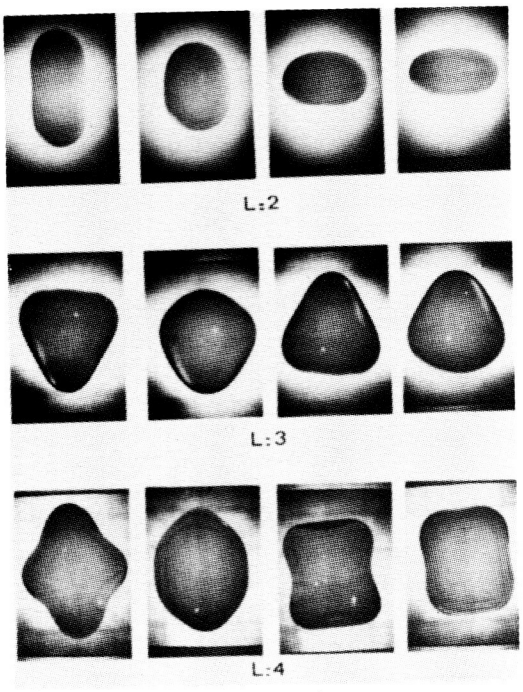

Figure 4

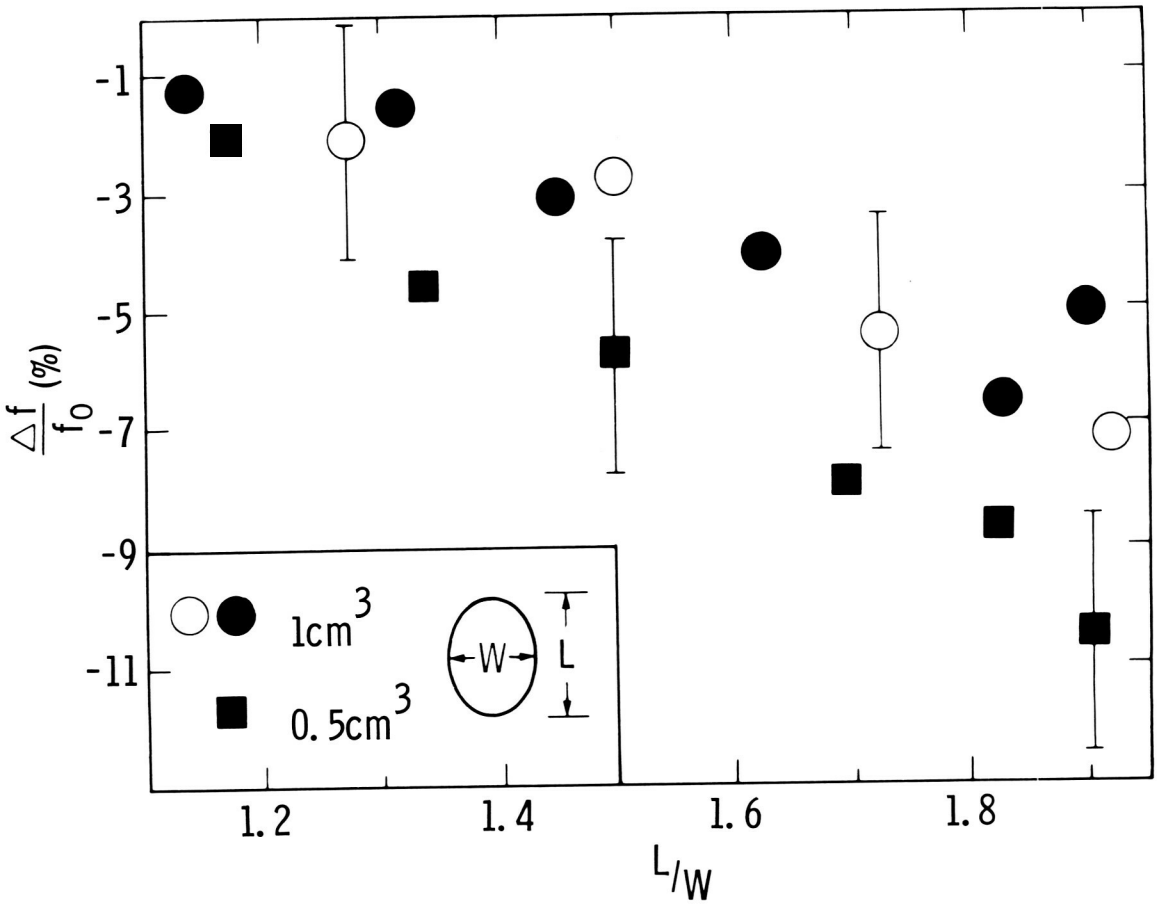

Figure 5

ORIGINAL PAGE IS
OF POOR QUALITY

ORIGINAL PAGE IS
OF POOR QUALITY

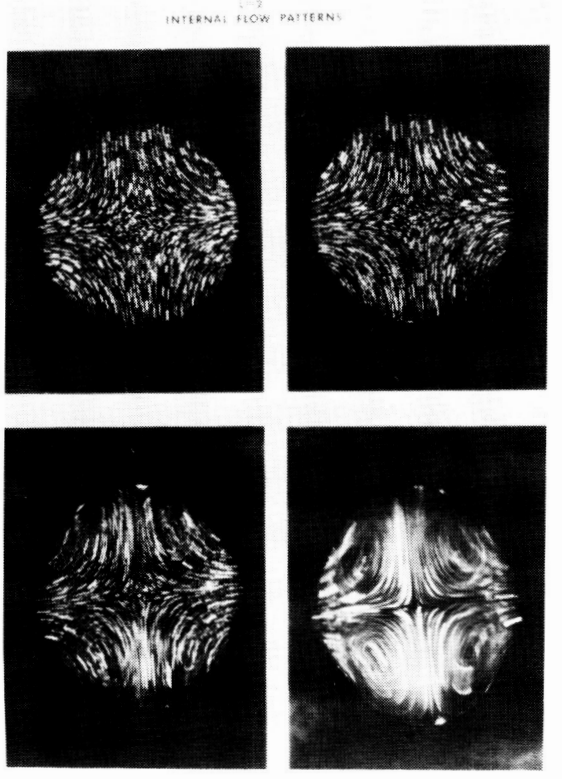

Figure 6

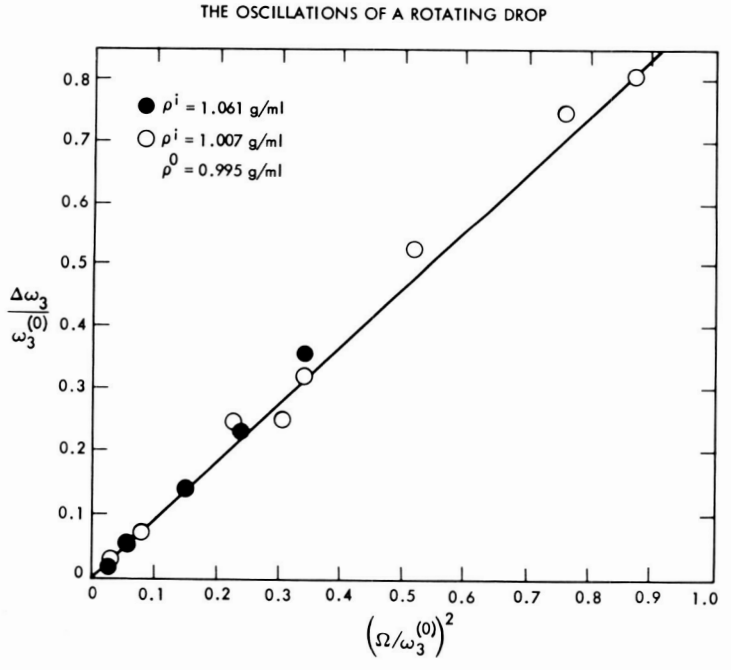

Figure 7

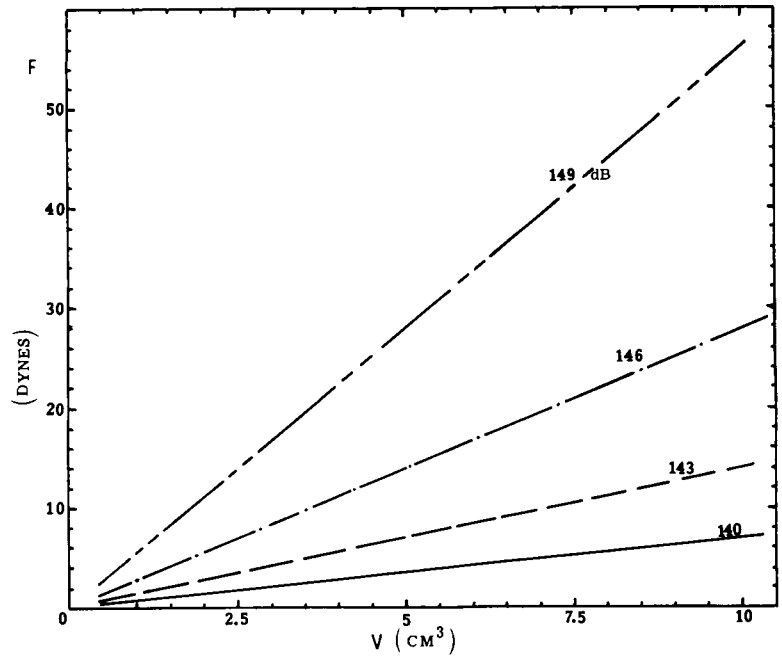

Figure 8

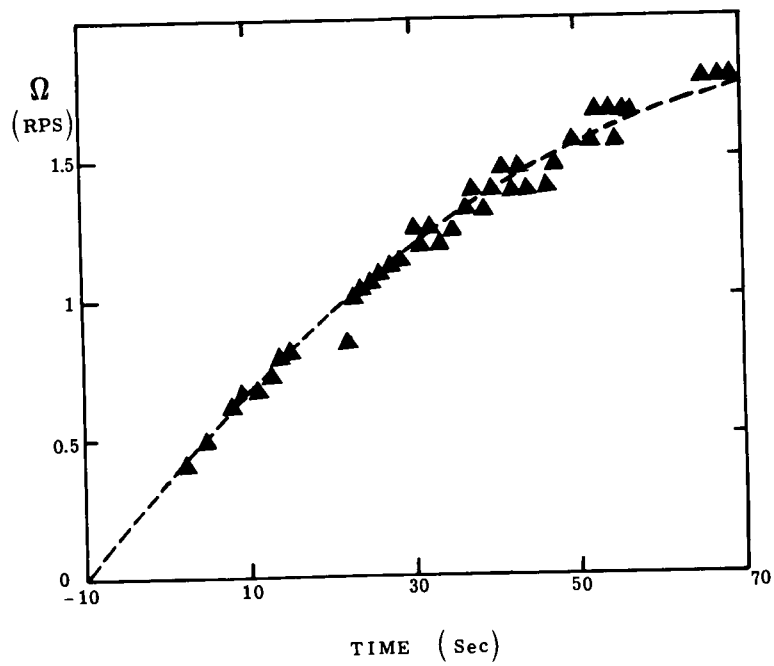

Figure 9

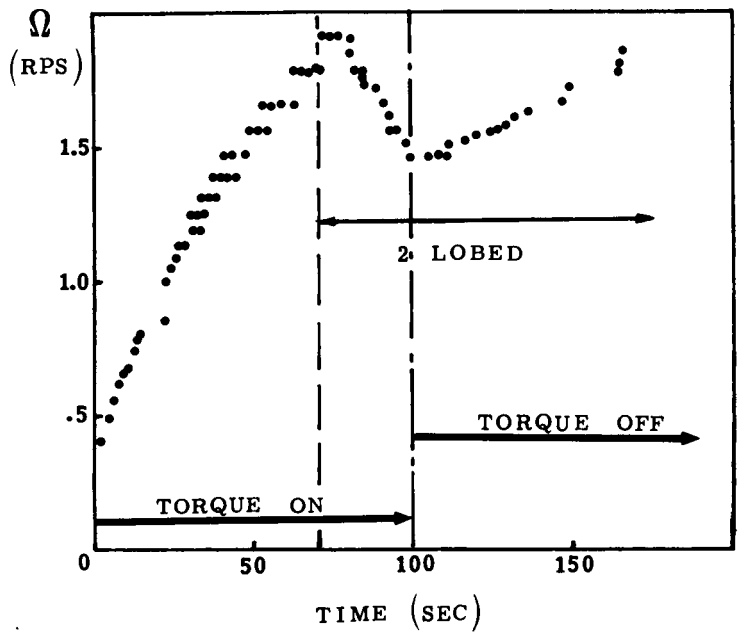

Figure 10

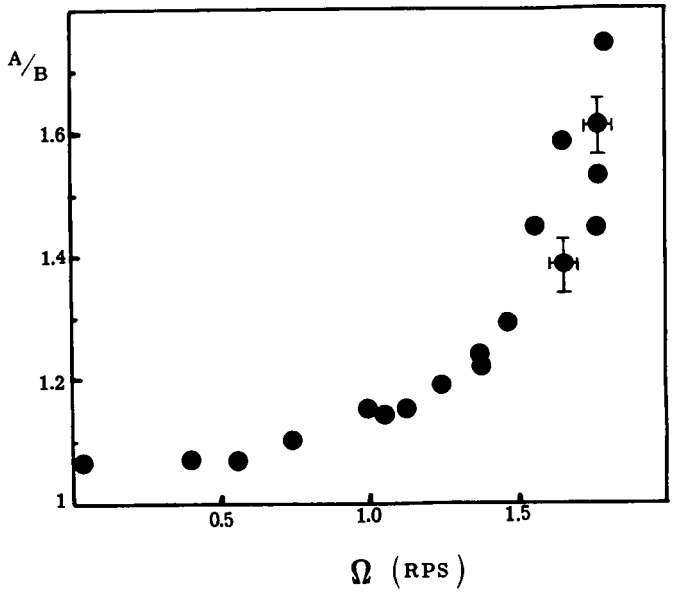

Figure 11

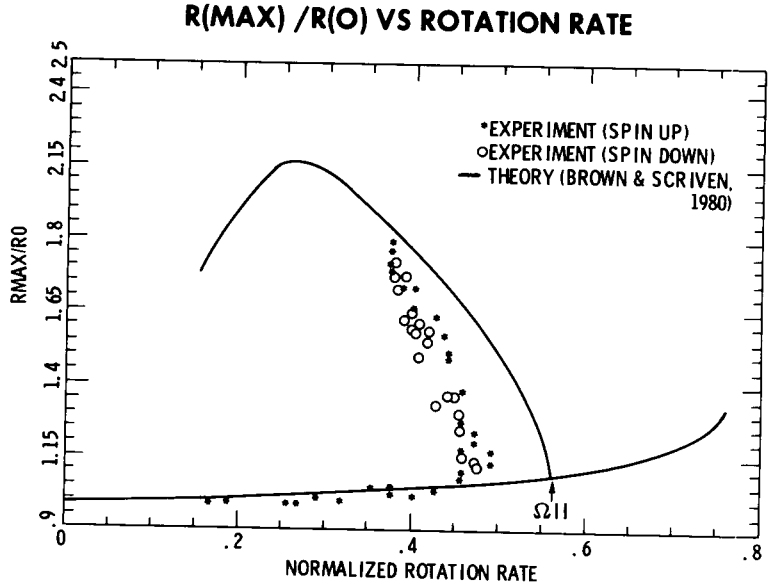

Figure 12

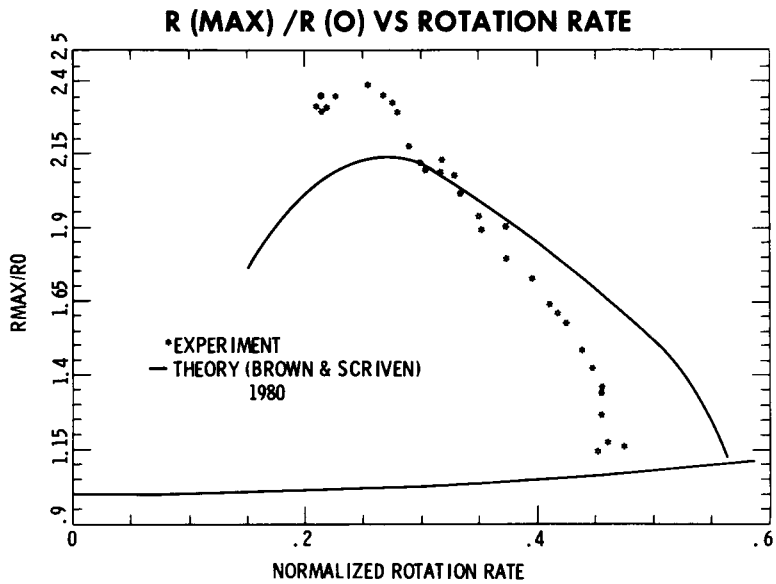

Figure 13

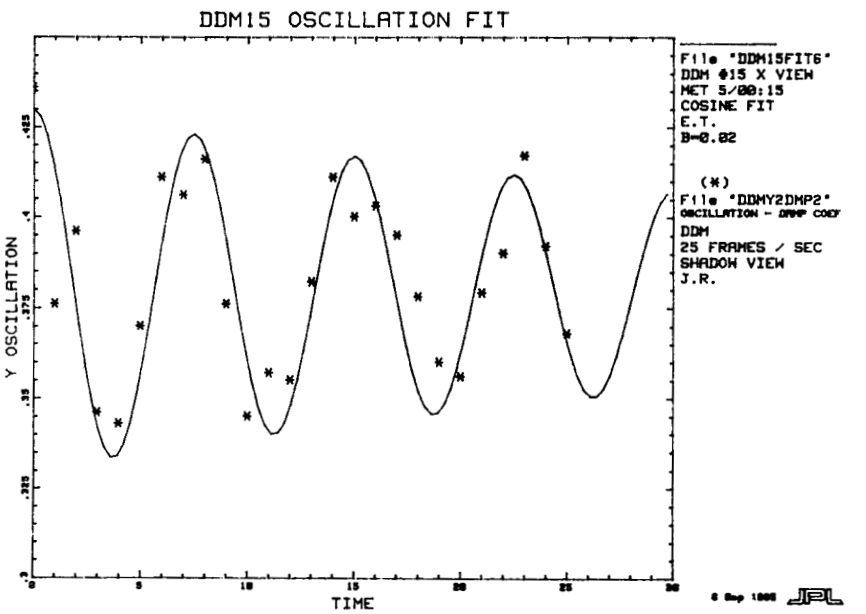

Figure 14

ORIGINAL PAGE IS
OF POOR QUALITY